The Thesis Committee for Jason Asher Goldberg
Certifies that this is the approved version of the following thesis:

Energy Balance Effects on MicroRNA Expression in a Mouse Model of Pancreatic Cancer

APPROVED BY
SUPERVISING COMMITTEE:

Supervisor: _____
Stephen D Hursting

Co-Supervisor: _____
Laura M Lashinger

Energy Balance Effects on MicroRNA Expression in a Mouse Model of Pancreatic Cancer

by

Jason Asher Goldberg, BS

Thesis

Presented to the Faculty of the Graduate School of

The University of Texas at Austin

in Partial Fulfillment

of the Requirements

for the Degree of

Master of Arts

The University of Texas at Austin

December 2010

Dedication

To my wife Megan, for your love, support, and understanding

Acknowledgements

I owe many people a great debt for the guidance, support, and love which was bestowed upon me during the writing of this thesis. I would like to thank Dr. Stephen Hursting for allowing me the opportunity to work in your lab as well as your mentorship and support. The time spent in your lab working with you and other members of the lab has been a rewarding experience. Though, I owe a great debt to all members of the Hursting lab for their assistance I would like to particularly thank Dr. Laura Lashinger for her guidance and patience in working with me. I also owe a debt to Dr. Shine Chang, Director of the UT-MD Anderson Cancer Center's R25 Cancer Prevention Research Training Program, funded by the National Cancer Institute, for her support as well as the funding I received from the training program. Finally, I would like to thank Dr. Randall Goldblum, whose support and guidance has played an integral role in my experiences thus far.

To my loved ones, I would like to thank you all for your patience and understanding. I owe a great debt to my wife who was with me every step of the way in the process being supportive and helping to keep my spirits up no matter how difficult I became. I would also like to thank my parents, grandparents, and siblings for their love and support, as well as their understanding of my obligations, which kept me away from family functions.

December 3, 2010

Abstract

Energy Balance Effects on MicroRNA Expression in a Mouse Model of Pancreatic Cancer

Jason Asher Goldberg, M.A.

The University of Texas at Austin, 2010

Supervisor: Stephen D Hursting

Co- Supervisor: Laura M. Lashinger

Pancreatic cancer is the fourth leading cause of cancer death in the United States, with a five-year survival rate under 5%. Given the disease's deadliness, increasing our understanding of the molecular nature of the pancreatic cancer is key to developing more effective preventive measures and treatments. Dietary energy restriction (DER) has been shown to have potent anticancer effects in pancreatic cancer, but the mechanism of action has yet to be completely elucidated. Here we investigate the potential of altered microRNA expression as a mechanism by which DER exerts its anticancer effect. Using the Exiqon microRNA Array, we identified several microRNAs of interest for further study. This includes microRNA (mir) 669c, a known regulator of glutathione-S transferases (linked to carcinogen metabolism and oxidative stress) that increases with age. To our knowledge, this is the first exploration of the effects of DER (which is known to suppress oxidative stress and other processes associated with aging and cancer) on microRNA expression. These findings may provide the initial steps towards identifying novel targets for pancreatic cancer prevention or treatment.

Table of Contents

List of Tables

List of Figures

Chapter 1: Introduction

In spite of its low rate of occurrence, pancreatic cancer is the fourth leading cause of cancer related death in the United States, with a five-year survival rate below 5% [1]. The deadliness of pancreatic cancer is in large part due to the difficulty of detecting the disease early and effectively treating it, particularly in the later stages when the disease is typically found. The inherent difficulty of early detection of pancreatic tumors means that upwards of 80% of all pancreatic cancer cases are diagnosed with metastases already present. This takes away the best treatment option, surgical resection of the tumor, which has a five-year survival of 20%[2] The low five-year survival of both surgical resection and other treatment options for pancreatic cancer helps to highlight its resilience in the face of current treatment options and the need for improved therapies, and particularly, prevention strategies.

Improving treatment and/or prevention options for pancreatic cancer depends on obtaining a better understanding of the molecular nature of the disease. Though much etiologic research on pancreatic tumorigenesis to date has been conducted *in vitro*, there is also a need for the development of relevant *in vivo* models to gain a better understanding of the disease. This will facilitate the development and assessment of novel treatments in a preclinical setting. For the purposes of our studies, we utilized a syngeneic transplant mouse model using NB508 and JC101 mouse pancreatic adenocarcinoma cell lines in wild-type FVB/N mice. The rationale behind the use of a pancreatic adenocarcinoma model is that adenocarcinomas account for 85% of all neoplasms in the pancreas, and thus represent the chief concern among tumors of the pancreas[3]. The NB508 line is derived from the Kras/INK4A transgenic mouse, which possesses a mutant K-ras and a heterozygous deletion for INK4A. These two genes are the most commonly altered in spontaneous human pancreatic adenocarcinoma, with K-ras activating

mutations present in ~85% of pancreatic tumors and INK4A deletions present ~80% of the time [2]. The JC101 line is derived from a K5.COX-2 transgenic mouse in which cyclooxygenase (COX)-2 is overexpressed in the pancreas under the keratin 5 promoter. The K5.COX-2 transgenic mouse serves as a model for inflammation-associated pancreatic cancer, specifically pancreatitis induced pancreatic adenocarcinoma [4]. Though the cell lines chosen have been used both in vitro and in vivo in the past, neither has been used in a subcutaneous transplant model.

Risk factors for pancreatic cancer include advanced age, smoking, chronic pancreatitis, diabetes, and obesity, with advanced age being the most significant [5]. Obesity is associated with a two-fold increased risk for an individual with a body mass index above 35 [6]. Better characterization of the obesity-pancreatic cancer association is of critical importance for 3 reasons: 1) other than smoking, obesity is the only other known modifiable risk factor for pancreatic cancer; 2) the growing obesity epidemic in America and throughout the world means it is likely that the number of cases of pancreatic cancer due to obesity will increase [7]; and 3) the fact that obesity enhances pancreatic cancer development suggests that examination of the link between obesity and pancreatic cancer could yield insight into the molecular targets and strategies for preventing or controlling this disease

In the context of energy balance (the biological homeostasis of energy in living systems), obesity represents a chronic surplus intake of calories relative to calories expended, which results in fat deposition and an alteration in serum hormones and growth factors associated with energy balance, cell proliferation and cell survival [8]. While obesity leads to a serum profile that promotes cellular proliferation, dietary energy restriction (DER) leads to a serum profile that is

consistent with reduced cellular proliferation and cell number homeostasis (Table 1).

	Obesity	DER	Cancer Risk
Insulin	Higher	Lower	Yes
Insulin-like Growth Factor-1	Higher (Biovailable)	Lower	Yes
Leptin	Higher	Lower	Yes
Adiponectin	Lower	Higher	Inhibitor

Table 1: Hormonal regulators of cell proliferation according to energy balance

DER is a dietary regimen that typically provides 70% of the calories but 100% of all micronutrients relative to an ad libitum-fed control group. The DER regimen thus prevents or reverses obesity without inducing malnutrition. In addition to preventing obesity and altering serum hormone profiles, DER has also proven in animal studies to be an effective tool to combat carcinogenesis [9]. In carcinogen-induced models of pancreatic cancer, DER was shown to suppress tumor formation [10], although the relevance of the carcinogen model is unclear. Dr. Lashinger of the Hursting lab has performed studies showing that DER decreases the severity and number of pancreatic ductal lesions in K5.COX2 transgenic mice when compared to the

control (Fig.1). Though energy balance modification is known to affect carcinogenesis, a complete understanding of the mechanisms involved has yet to be obtained.

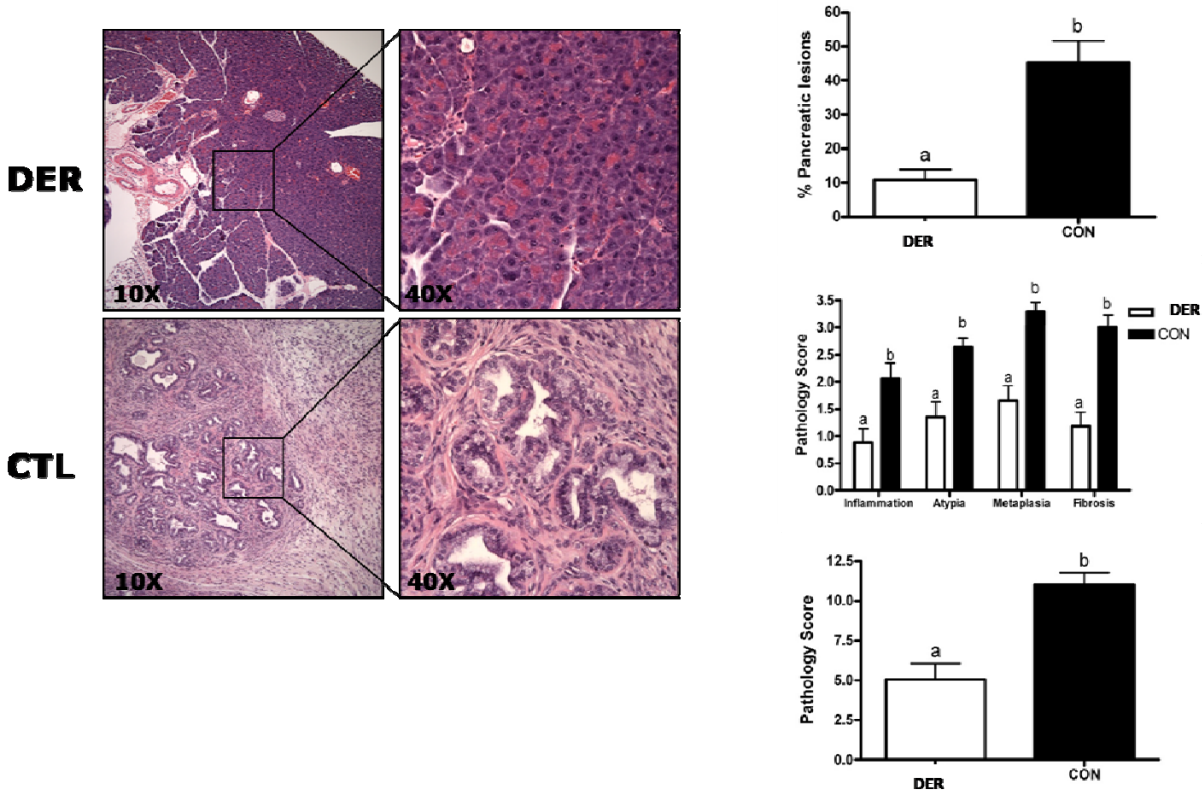

Figure 1: Histological analysis of pancreatic ductal lesion in BK5.COX-2 transgenic mice shows that DER Protect from the formation of pancreatic lesions when compared to pancreas from BK5.COX-2 mice on control diet. Pancreata were also scored for inflammation, nuclear atypia all of which were reduced in BK5.COX-2 mice DER when compared to control diet.

Despite their growing importance in regulating translation, the role of microRNAs (miRNA) in the anti-cancer effects brought about by DER are unknown. First discovered in *C. elegans*, microRNAs (miRNAs) are small non-translated RNA molecules with an average length of twenty-two nucleotides. Initially believed to be a novel finding confined to worms, interest in them began in earnest with the identification of let-7 miRNA as well as the observations that is phylogenetically conserved. In the decade following identification of let-7, more than 700 human miRNA genes have been identified and their importance as posttranscriptional regulators of gene

expression has emerged. Current estimates have miRNA playing a role in regulating up to 30% of human genes involved in a range of cellular processes including: cell cycle, differentiation, and development [11].

Given the scope and diversity of miRNA regulation in cells, it is not surprising that research has implicated abnormal miRNA profiles as a contributing factor to a host of human diseases, including cancer and metabolic syndrome [12, 13]. To date a number of studies have been performed on paraffin-embedded pancreatic tumor samples in an attempt to create a comprehensive list of miRNAs that are altered in pancreatic cancer. *In vitro* studies have identified a role for miRNA play in pancreatic cancer [14]. Other studies have looked at adipose and other tissues from obese patients who suffer from metabolic syndrome and found inappropriate expression profiles for miRNA. However, the relationship between altered miRNA expression and health problems associated with obesity, such as pancreatic cancer, has yet to be established. *Given that improper miRNA expression plays a role in pancreatic cancer and metabolic alterations associated with obesity, I hypothesized that tumors in mice on DER, relative to ad libitum-fed controls, will exhibit favorable changes in miRNA expression that help to explain the DER-associated decrease in tumor burden.* The aims of this thesis project are:

Specific Aims

Aim 1. Establish the appropriateness of using a subcutaneous syngeneic transplant model to study the anti-cancer effects of DER. FVB mice will be placed on either a control diet or DER for 7 weeks prior to injection with $2x10^5$ JC101 or NB508 cells. Following 4-weeks of tumor growth, mice will be killed, and tumors, blood and other tissues collected. Endpoints

measured will include body weight, tumor burden, serum hormone profile, and immunohistochemistry (IHC).

Aim 2. Determine changes in miRNA expression in tumors from mice on DER, relative to control diet. The miRNA expression of tumors from control and DER mice that received JC101 injection (but not the NB508 cells, which were unresponsive to DER in Aim 1 studies) will be assessed using the Exiqon array system. Array data will be confirmed using the Taqman RT-PCR system for miRNA. Additionally, *in vitro* studies will be performed exposing the JC101 cell line to serum starvation and IGF-1 treatments in an attempt to identify miRNA changes influenced by energy balance or IGF-1 modulation.

Chapter 2: Methods

Mouse Study Design

Upon receipt, 40 FVB mice (Charles Rivers Laboratories) were singly housed, placed on chow diet and allowed one week for acclimation. Following this acclimation period, mice were randomized to receive either the control or DER diet regimen (20 mice/diet treatment) as further described below in the diet manipulation portion of the methods section. Additionally, the mice had their body weights recorded and were given nestlets weekly for the duration of the study. The mice were maintained on diets for seven weeks prior to a subcutaneous injection of NB508 or JC101 mouse pancreatic cancer cells. Following the injection of tumor cells, the mice remained on their respective diets and were monitored as outlined below.

Syngeneic Subcutaneous Transplant:

NB508 and JC101 cells were separately suspended (in DMEM media containing 10% FBS) to a concentration of 2 million cells cells per ml. Half of the mice (n=20) received a subcutaneous injection of $2x10^5$ NB508 cells with the remainder receiving $2x10^5$ JC101 cells. Mice were palpated biweekly for tumor formation. Upon detection of tumors, they were measured by electronic caliper three times/week. Tumors grew for four weeks post-transplant until 50% of tumors measured greater than 1cm diameter, at which time all mice were killed. During euthanasia, mice were anesthetized using isoflurane. Upon anesthetization, a cardiac puncture was performed as a terminal blood draw after which a cervical dislocation was performed. Collected blood was allowed to sit at room temperature for thirty minutes, and then spun for 5 minutes at 13,000 RPM to separate serum from the blood. The serum was collected and placed on dry ice. Tissues collected from the euthanized mice included tumor, normal pancreas, liver, and visceral white adipose tissue.

Diet Manipulation

Upon arrival, mice (n=40) were placed on a chow diet for one week to allow for acclimation to the new environment. Following acclimation, all mice were placed on the control diet (AIN-76A; Research Diets #D10001) for one week. Mice were then randomized to receive one of two diet treatments (n=20): 1) Control Diet; or 2) 30% DER (Research Diet #D09071302),. Mice remained on their respective diet for the remainder of the study (additional information on diets can be found in the appendix 1). Food intake for mice placed on the AIN-76A control diet had their food intake measured weekly in order to calculate the daily food allotment for the mice on 30% DER. Briefly, food intake for each singly housed mouse was measured by subtracting the weight of the remaining food from the initial food given. Individual food intake for all mice on the AIN-76A diet was used to calculate the daily food administered to DER mice using the following equation:

$$\text{Daily Food Allotment (g) for DER mice} = \frac{0.7x\ AIN{-}76A\ Average\ Food\ Intake(g)}{7\ days}$$

CD31 Immunohistochemistry

Tumor tissue sections were fixed in 10% formalin for twenty-four hours after which the samples were transferred to 70% ethanol. The tumor samples were then transported to the histology core at M.D. Anderson Science Park where they were embedded in paraffin. In order to stain for CD31, slides were placed in a 60^{o}C oven for thirty minutes. Following incubation, slides were deparraffinized by placing them in Hemo-De for five minutes (twice), 100% Ethanol for five minutes (twice), 95% Ethanol five minutes (once), and then being rinsed under running water. The slides were then placed in 3% H_2O_2 water for ten minutes after which time they were rinsed in water. Following the rinse, the slides were paped and the tissue was covered with Tris buffer. The slides were then incubated in 0.06% Protease in Tris for ten minutes, after which

they were rinsed and then blocked in TNB buffer for thirty minutes. The slides were then incubated with primary antibody using Pharmingen anti-CD31 (Clone MEC 13.3) monoclonal antibody. The primary antibody was diluted 1:400 in TNB buffer and then incubated for at least one hour at room temperature (overnight incubation is recommended). Following primary antibody incubation, the slides were placed in PBS for ten minutes with T/A in preparation for a thirty minute incubation with the secondary antibody (Biotinlyated anti-Rat IgG) diluted at 1:200 in TNB. Following the secondary incubation, the slides were washed for ten minutes in PBS with T/A and then incubated for thirty minutes in SA-HRP diluted 1:100 in TNB buffer. The slides were washed again in PBS with T/A for ten minutes before incubating the slides for ten minutes in biotinylated tyramide (diluted 1:50 in 1x Amplification Diluent). Then the slides were washed again in PBS with T/A this time for fifteen minutes, incubated with SA-HRP (1:100 in TNB Buffer), and then washed in PBW with T/A for 10 minutes. To develop the slides Sigma Tablet DAB were used. During the development of the slides they were washed, counterstained, cleared and coversliped with a permanent mounting media.

Ki-67 Immunohistochemistry

To stain for Ki-67, a marker of cell proliferation, the fixed and embedded tumor tissue (described above) was deparaffinized in xylene and hydrated in graded alcohols (100%, 95%) to water. Endogenous perxoidase activity was then blocked using a wash in 3% H_20_2 for 10 minutes. The slides were then washed and antigen was retieved by microwaving the samples in a microwave with 10mM Citrate Buffer pH 6.0 for 15 minutes (10 minutes at full power and five at 50%) followed by a twenty-minute cool down and wash. Next, the slides were blocked with non-specific antibodies by incubating them with Biocare Blocking Reagent for ten minutes. Following blocking, the slides were drained and incubated overnight at 4^oC with primary

monoclonal Ki-67 antibody (Dako#M7240) at a dilution of 1:50. After incubating overnight the slides were washed in buffer for 5 minutes, changing the buffer once, and then incubated for fifteen minutes at room temperature with biotinylated rabit-anti-mouse F(ab)' (Accurate Chem) at a 1:250 dilution. The slides were then washed for five minutes in buffer, before being incubated with SA-HRP (BioGenex) for thirty minutes at room temperature. Another five minute buffer wash was performed and the slides were incubated with Dako DAB until staining developed at which time the slides were washed, counterstained, dehydrated, and then coverslipped for viewing.

Caspase 3 Immunohistochemistry

To stain for Caspase 3, tumor tissue was deparaffinized in xylene and hydrated in graded alcohols (100%, 95%) to water. Endogenous peroxidase activity was then blocked using a wash in 3% H_20_2 for ten minutes. The slides were then washed and antigen was retrieved by microwaving the samples in a microwave with 10mM Citrate Buffer pH 6.0 ten minutes followed by a twenty-minute cool down and wash. Next, the slides were blocked with non-specific antibodies by incubating them with Biocare Blocking Reagent for ten minutes. Slides were then drained and incubated at room temperature for thirty minutes with primary Caspase-3 polyclonal antibody (R&D AF835) at a 1:2000 dilution. Following incubation the slides were washed with buffer for ten minutes and then incubated for thirty minutes at room temperature using biotinylated goat-anti-rabbit IgG (Vector) at 1:500 dilution followed by a ten minute buffer wash. The slides were then washed for five minutes in buffer, before being incubated with SA-HRP (BioGenex) for thirty minutes at room temperature. After another 10 minute buffer wash the slides were incubated with BioGenex DAB until staining developed at which time the slides were washed, counterstained, dehydrated, and then coverslipped for viewing.

Serum Hormone Analysis

Serum hormone analysis was performed using Milliplex Map Kits (Millipore, Buillerica, MS) and a Bioplex 200 system (Bio-Rad, St. Louis , MO) to measure serum levels of insulin, IGF-1, leptin, and adiponectin. Serum was obtained from blood collected during sacrifice of JC101 mice on control diet (n=10) and DER (n=9) . All procedures were performed using manufacturer's instructions.

Initial Assessment of Exiqon miRNA Array

We had not previously used the Exiqon array system as a tool to detect changes in miRNA expression in our model. Thus, a small pilot study (limited to one randomly selected mouse per diet treatment due to expense) was initiated to confirm the utility of this array platform for testing our hypothesis. Frozen tumor and pancreas from these two mice were processed using the mirVana Total RNA extraction kit as described below. Total RNA was then quality checked using the Agilent 2100 Expert Bioanalyzer (Agilent Technologies, Inc.; Santa Clara, CA) prior to running the Exiqon arrays. Four paired arrays were run with the following comparisons being made: 1.) Control Tumor/Control Pancreas, 2.) DER Tumor/DER Pancreas, 3.) DER Pancreas/Control Pancreas, and 4.) DER Tumor/Control Tumor. All arrays were run following the procedure described below.

Total RNA extraction from tumor tissue

Following euthanasia, tumor tissue was extracted and flash frozen in liquid nitrogen and stored at -80^{o}C. The extraction of RNA from tumor tissue was performed using the mirVana miRNA isolation kit (Applied Biosystems #AB1560). Tumor tissue was placed on dry ice wrapped in foil and a section of approximately 150mg was collected, diced, and placed in a 50ml conical tube. Additionally, lysis/binding buffer was added at ten volumes per 0.1g of tissue (1ml per 100mg of tissue) to the 50ml conical tube, and the samples were mechanically homogenized

using a Rotor-Stator homogenizer. Following homogenization, miRNA Homogenate Additive was added to the samples at 1/10th volume of the added lysis/binding buffer and vortexed for 30 seconds. Samples were placed on ice for 10 minutes and then transferred to a 15ml conical containing with acid phenol chloroform (volume equal to the lysate volume before addition of miRNA homogenate) and vortexed for 30 to 60 seconds. The vortexed lysate/chloroform samples were then spun for five minutes at maximum speed and room temperature. After centrifugation, the aqueous phase was carefully removed (the volume noted) and placed in a new 15ml conical with 100% Ethanol (1.25 volumes of removed aqueous phase). The provided filter cartridges were placed in a collection tube and the lysate/ethanol mixture (up to 700ul) was pipeted in and centrifuged for ~15 seconds at no more than 10,000xG (to avoid damaging the filter). Following the spin, the flow through was dumped and the process repeated until all of the lysate/ethanol mixture had been run through the filter. After running the samples through the filters, a series of three washes were performed: (1) 700 ul of Wash Solution 1; (2) 500 ul of Wash Solution 2/3; and (3) 500 ul of Wash Solution 2/3. Following each wash, tubes were spun at no more than 10,000xg for 10 seconds and the flow through was discarded. After performing the three washes, filter and collection tubes were spun for one minute (at under 10,000 xg) and the filter was transferred to a new collection tube. Finally, 100ul of 95^{o}C nuclease-free water was placed on the filter, which was spun for 20-30 seconds at maximum speed. Following the spin, the filter cartridge was disposed of and the collected total RNA was stored at stored at -80^{o}C.

microRNA array of tumor tissue

Total RNA extract from the tumor tissue of mice on DER and control diet were matched. The quality of the total RNA was assessed using the Agilent 2100 Expert Bioanalyzer (Agilent Technologies, Inc.; Santa Clara, CA). Upon confirmation of the quality, samples were labeled

using the Exiqon miRCURY LNA™ microRNA Power Labeling Kit (Exiqon Inc.; Woburn, MA). 1μg of total RNA for each sample was dephosphorylated and labeled with Hy3™ or Hy5™ dyes, then combined and hybridized to miRCURY LNA™ Arrays, version 15.0 (Exiqon, Inc.) on the TECAN HS400Pro hybridization station (Tecan US, Inc., Raleigh, NC). The control RNAs (so-called "spike-in") were included in the labeling and hybridization to assist in setting scanner parameters. The array slides were scanned on the GenePix 4200 scanner (Axon Instruments; Gaithersburg, MD) and analyzed with GenePix Pro version 6.0 software (Axon Instruments).

IGF-1 treatment of Panc02 cells and total RNA extraction

Panc02 cells were grown in a T-175 flask in DMEM media with 10% FBS until confluent. The evening before IGF-1 treatment, Panc02 cells were trypsinized, spun down, washed in PBS, and resuspended in 30 ml of DMEM media with 10% FBS. 1ml of the resuspended Panc02 cells was added to each well in the six well plate in addition to 1 ml of media. The next morning all six wells were washed in PBS and incubated in serum free DMEM for four hours prior to treatment. The treatment groups were DMEM media with 10% FBS, serum free DMEM media, and 1, 2, 4 or 8 hour exposure to IGF-1(400ng/ml ,equivalent to the typical serum levels observed in mice consuming a control diet). Following completion of the time points, the media was aspirated, wells were washed with PBS, and then trypsinized with 1ml of trypsin for five minutes at 37^{o}C. After incubation 1ml of DMEM media with 10% FBS was added to each well. The trypsinized cells were transferred to 15ml conical tubes and spun down for five minutes at 1500 RPM. The media was then aspirated off and cells were resuspended in 1 ml of PBS, transferred to a 2ml eppendorf tubes, and spun again for five minutes at 1500 RPM. The PBS was aspirated and isolation of total RNA was preformed using

mirVana miRNA isolation kit (Applied Biosystems #AB1560). The resulting cell pellet was resuspended in 500ul of lysis/binding buffer and vortexed for 15seconds. 50ul of miRNA homogenate additive was then added to the solution, vortexed for 30 seconds, and samples were placed on ice for 10 minutes, and then transferred to a 15ml conical tube containing acid phenol chloroform (volume equal to the lysate volume before addition of miRNA homogenate) and vortexed for 30-60 seconds. The vortexed lysate/chloroform samples were then spun for five minutes at maximum speed and room temperature. After centrifugation, the aqueous phase was carefully removed (volume noted) and placed in a new 15ml conical with 100% ethanol (1.25 volumes of removed aqueous phase). The provided filter cartridges were placed in collection tubes and the lysate/ethanol mixture (up to 700ul) was added and centrifuged for ~15 seconds at no more than 10,000xg (to avoid damaging the filter). Following the spin, the flow through was dumped and the process repeated until all of the lysate/ethanol mixture was run through the filter. After running the samples through the filter, a series of three washes were performed: (1) 700 ul of Wash Solution 1; (2) 500ul of Wash Solution 2/3,; and (3) 500 ul of Wash Solution 2/3. Following each wash, tubes were spun at no more than 10,000xg for ten seconds and the flow through was discarded. After performing the three washes, filters and collection tubes were spun for one minute (at under 10,000 xg) and the filters were transferred to a new collection tube. Finally, 100ul of 95^{o}C nuclease-free water was placed on the filter, which was spun for 20-30 seconds at maximum speed. Following the spin, the filter cartridge was disposed of and the collected total RNA was stored at -80^{o}C.

Reverse Transcription of Targeted microRNA from Total RNA Extract

The concentration of total RNA collected using mirVana miRNA isolation kit (Applied Biosystems #AB1560) was assessed using a ND-1000 spectrophotometer (Nanodrop). Total RNA samples were then diluted to a concentration of 2ng/ul in preparation for reverse transcription using the TaqMan MicroRNA Reverse Transcription Kit (Part # 4366596 or 4366597). Five ul of the diluted total RNA was combined with 7ul of master mix in a 0.2ml PCR tube for each 15ul reaction desired to take place. 3ul of appropriate RT primer (Applied Biosystems) for the miRNA of interest was then added to each tube. The tubes were gently misted, centrifuged, and allowed to sit on ice for five minutes. Following the resting period, the samples were placed in a thermocycler (Eppendorf MasterCycler EP gradient S) using the programmed steps below:

Step Type	Time (min)	Temp (^{o}C)
Hold	30	16
Hold	30	42
Hold	5	85
Hold	∞	4

The RT samples were stored at -20^{o}C prior to PCR. PCR for miRNA's of interest was preformed using Taqman Probes from Applied Biosystems and Taqman Universal Master Mix II, no UNG (Applied Biosystems #4440043). Each PCR reaction requires 10ul of the master mix, 7.67ul of nuclease free water, 1.33ul or the appropriate RT reaction, and 1ul of the appropriate PCR primer. The 96 well plate to perform PCR was sealed with an optical adhesive cover and

then pulse centrifuged to spin down the contents and eliminate air bubbles. To perform PCR, an eppendorf realplex^4 mastercycler EPgradientS was used with the programmed steps below:

Step	Enzyme Activation	PCR	
	Hold	Cycle (40x)	
		Denature	Anneal/ Extend
Time	10 min	15 sec	60 sec
Temp(°C)	95	95	60

Statistical Analysis

Statistical analysis was preformed on all data using PASW Statistics 17 (formerly SPSS). Statistically significant differences in body weights, caloric consumption, as well as all serum hormone levels were calculated using paired sample t-tests. Analysis of the tumor burden required the use non-parametric Mann–Whitney U test in order to determine significance. Assessment of miRNA expression was carried out utilizing a single sample t-test in which the relative quotients of expression was compared to a test value of 0.

Histopathologic Analysis

Formalin-fixed pancreatic tissue from BK5.COX-2 mice were embedded in paraffin and cut into 4-um thick sections and processed for hematoxylin and eosin (H&E) staining. The percentage of the pancreas comprised of proliferating ducts was determined under low power magnification using H&E-stained sections. Metaplastic changes in ducts (metaplasia), cellular and nuclear atypia (atypia), degree of inflammatory cell infiltration (inflammation), and relative

size of the stroma and level of fibrosis (fibrosis) were scored in a blinded manner by a certified veterinary pathologist (M.J.M.) according to the following criteria. 0= normal pancreas, 1= minimal (5-10% affected), 2= mild (10-25% affected), 3=moderate (25-50% affected), 4= marked (>50% affected). These indices of pathology were also combined to give a composite score of severity for each mouse.

Chapter 3: Results

Effects of DER on Pancreatic Tumor Growth

Following a 7-week diet treatment period that resulted in lean DER mice (mean JC101:19.4 ±0.45 g and NB508:19.3±0.057g; Figure 2a,b) relative to control mice (mean JC101: 27.4+0.75g and NB508: 28.1±0.43g; Figure 2a,b). Mice were injected with either JC101 or NB508 pancrearic cancer cell lines and the tumors were followed for four weeks, at which time all mice were killed and tumor tissue, blood through a cardiac puncture, and their pancreata were collected. As expected, analysis of tumors collected showed that DER, relative to control diet, decreased tumor burden (464.7±101.32 mg in DER versus 964.8±93.21mg in controls, p=0.007; Figure 2e) in mice that received JC101 cells. However, no diet effect was observed in mice injected with NB508 cells (239.4±126.65 mg in DER versus 208.5±51 mg in Controls, p=0.48 Figure 2f). The failure of the NB508 arm of the study is surprising given past successes with the cell line in the Hursting lab. Notably the NB508 cells injected did not behave as aggressively as they have in past studies when they were othotopically injected into pancreata, which may indicate that the cell line is not suitable for a subcutaneous study or requires modifications to the protocol, such as the addition of matrigel or higher cell concentrations. While this warrants further investigation, all subsequent studies in this thesis will focus on the JC101 cells, which were responsive to DER in our study.

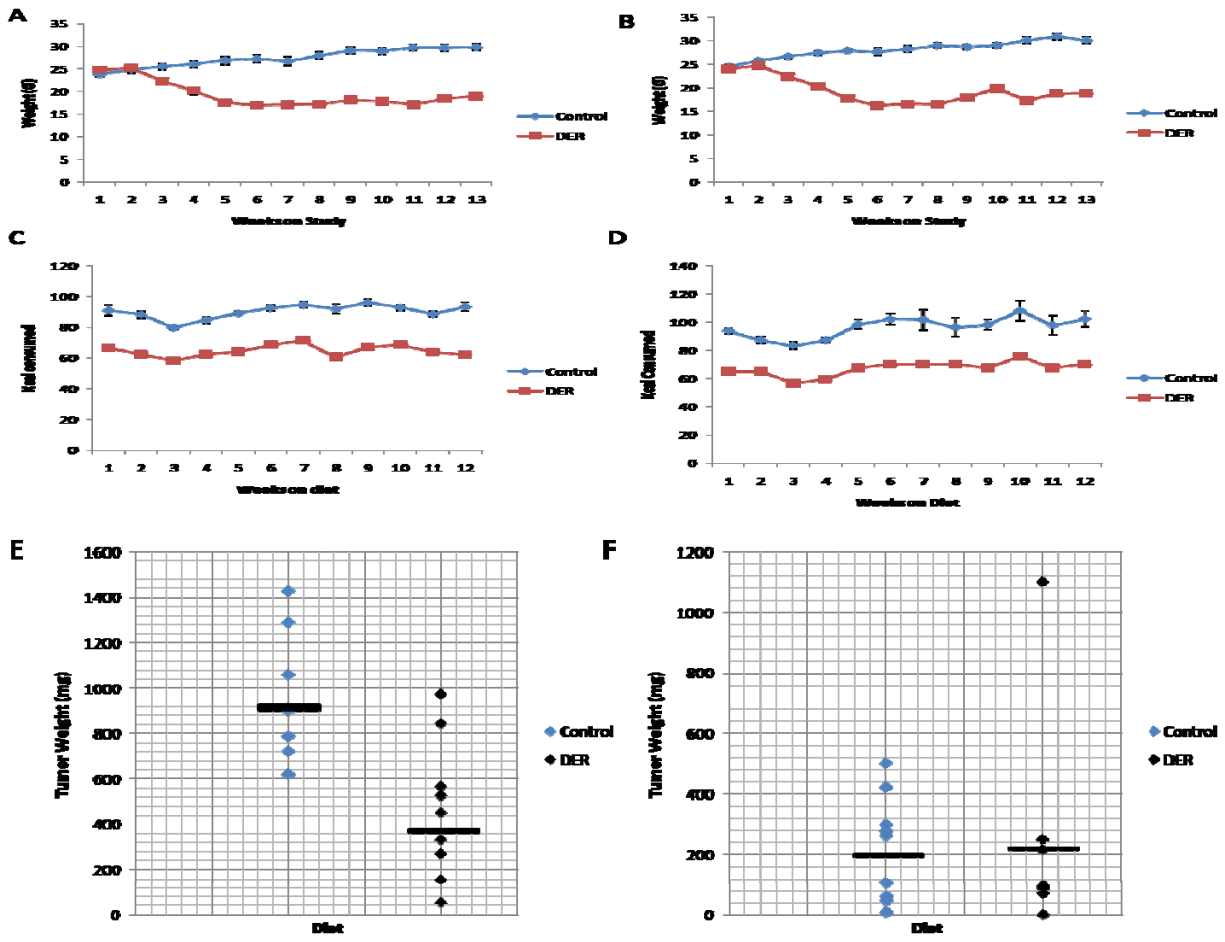

Figure 2: Animal Study Data: Weight, Calorie Consumption, Tumor Burden. A.) Body weight for mice that received JC101 cells ($p<0.0001$). B) Body weight for mice the received NB508 cells ($p<0.0001$) C.) kCal consumed for mice that recived JC101cells ($p<0.0001$) D.) kCal consumed for mice that received NB508 ($p<0.0001$) E.) Tumor Burden for mice with JC101 cells average weight 964.75±93.21 mg for mice on control diet and 464.6667±101.32 mg for mice on DER ($p=0.007$) F.) Tumor Burden for mice with NB508 cells average weight 208.51 ±51 mg for mice on control diet and 239.375±126.65 mg for mice on DER ($p=0.477$).

Effects of DER on Serum Hormones and Immunohistochemical Markers

Further characterization of the effect of of DER in mice that received JC101 cells was performed using serum analysis from the terminal bleed and immunohistochemistry on collected tumor tissue. Serum analysis was preformed using Millipore hormone assay kits to assess levels of IGF-1, insulin, adiponectin, and leptin. Mice placed on DER showed the expected significant

changes in serum levels of insulin, IGF-1, and leptin (Figure 3a,b,c). While serum adiponectin levels were not significantly different, they did trend in the expected direction (Figure 3d).

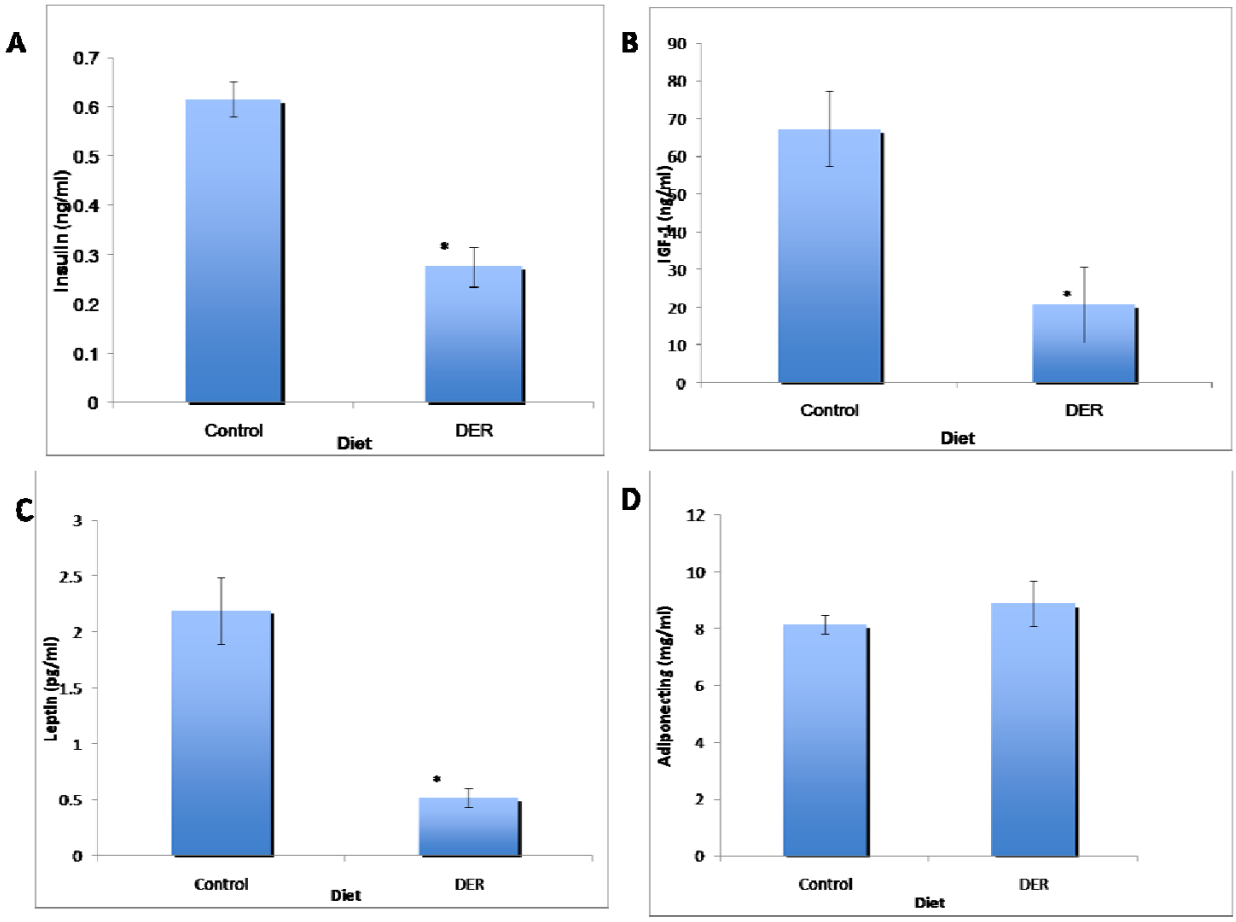

Figure 3: Analysis of serum hormones from mice that received an injection of $x10^5$ JC101 cells. A.) The average concentration of insulin in the analyzed serum was 0.71 ng/ml in control mice and 0.28 ng/ml in DER mice (p= 0.014) B.) IGF-1 was present at a concentration of 67.21 ng/ml in control mice and 20.70 ng/ml in DER mice (P < 0.0001). C.) Leptin serum levels were 1.99 pg/ml in control mice and 0.52 in DER mice (p=0.0005) D.) Adiponectin was only slightly lowered in control mice, 8.13 ng/ml, compared to DER mice, 8.89, yielding a non-significant difference (P=0.378) that trended in the expected direction.

Slides were made from paraffin-embedded blocks of tumor tissue and stained for H&E, CD31, Ki67, and cleaved caspase 3 in order to assess the general structure and vascularization of the tumors as well as assess DER effects on cell division and apoptosis. Analysis of the slides shows that DER decreased fibrosis, cellular proliferation, and vascularization in the tumors when compared to control tumors, while not affecting the rate of apoptosis (Fig.4). The alterations in

the general biology of the tumor in response to DER are consistent with previous findings in the Hursting lab in several cancer models.

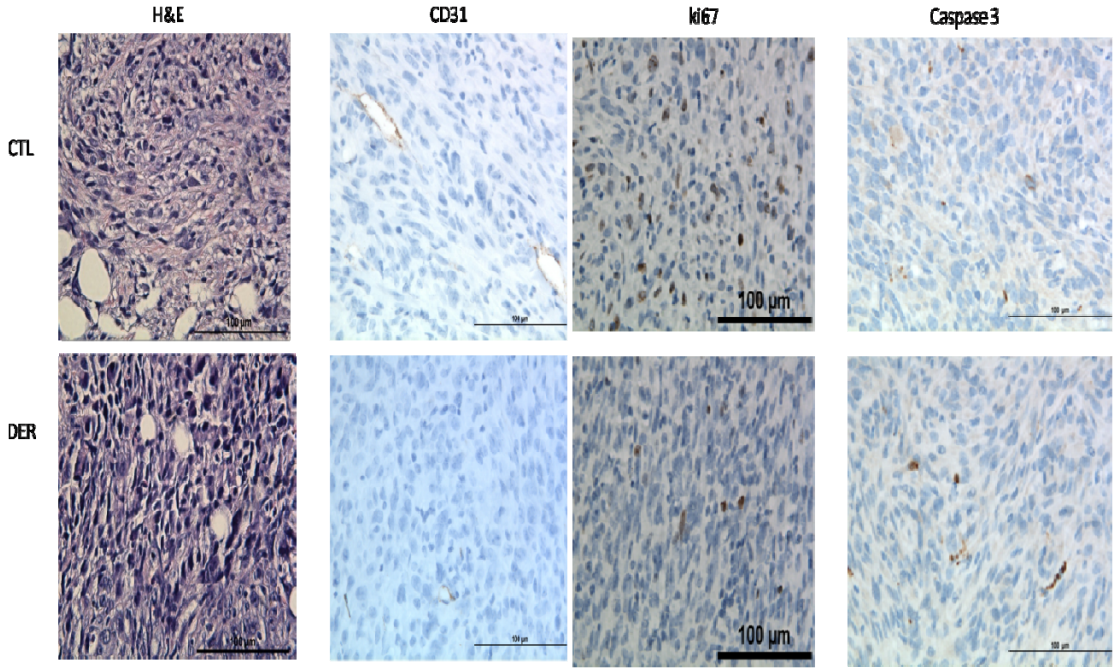

Figure 4: Immunohistochemistry was preformed on slides prepared from paraffin-embedded tumor tissue collected from JC101 mice during sacrifice. H&E staining was performed to assess the gross pathological features of the tumor, and shows a decrease in fibrosis in DER mice when compared to control. CD31 staining was performed to evaluate differences in vascularization between control and DER tumors. As seen in the slides imaged there is an increase in vascularization in control tumors compared to that seen in DER tumors. Ki-67 and Caspase 3 staining were performed to assess rates of cellular proliferation and apoptosis respectively. DER tumors displayed a decreased Ki-67 staining indicative of lower rates of cellular proliferation while not displaying any change in apoptosis when compared to control tumors. All images were captured at 40x magnification.

Effects of DER on miRNA Expression

The unexplored nature of the relationships between DER modulation, miRNA expression, and tumor burden necessitated a global approach to identify potential miRNA for further investigation. Before using a large amount of tumor tissue and funding, we decided to perform a pilot to assess the usefulness of the Exiqon array system using tumor and pancreas tissue from one control and one DER mouse. Four comparisons were chosen to determine the effects of DER (relative to control), as well as the effects of cancer development (versus normal

pancreas tissue) on miRNA expression. The two conditions that yielded the largest number of differentially expressed miRNA were: Control Tumor v. Control Pancreas and DER Tumor v. DER Pancreas. Although limited by the small sample size, these pilot data showing differentially expressed miRNAs between tumor and normal pancreas, and between DER and controls, were encouraging.

Table 2

miRNA	Relative Quant (Tumor Control / Pancreas Control)	Pos Error	Neg Error
mmu-miR-763	**0.0359**	0.011	0.008
hsa-miR-452	**0.0588**	0.012	0.010
kshv-miR-K12-8	**0.0596**	0.017	0.013
hsa-miR-221*	**0.0597**	0.013	0.010
hsa-miR-148a/mmu-miR-148a	**0.0661**	0.010	0.008
hsa-miRPlus-E1053	**0.0883**	0.011	0.010
hsa-miRPlus-F1193	**0.0938**	0.426	0.077
hsa-miR-375/mmu-miR-375/rno-miR-375	**0.1054**	0.021	0.018
hsa-miR-802/mmu-miR-802/rno-miR-802	**0.1180**	0.010	0.009
rno-miR-494	**0.1279**	0.011	0.010
hsv1-miR-H7*	**0.1346**	0.008	0.007
mmu-miR-675-5p/rno-miR-675	**0.1358**	0.017	0.015
hsa-miR-200c/mmu-miR-200c/rno-miR-200c	**0.1424**	0.034	0.027
mcmv-miR-m88-1	**0.1497**	0.049	0.037
hsa-miR-525-5p	**0.1584**	0.032	0.027
hsa-miR-665	**0.1703**	0.011	0.011
hsa-miRPlus-F1099	**0.1875**	0.107	0.068
hsa-miR-200b/mmu-miR-200b/rno-miR-200b	**0.1909**	0.052	0.041
hsa-miR-200a/mmu-miR-200a/rno-miR-200a	**0.1924**	0.058	0.045
hsa-miR-410/mmu-miR-410/rno-miR-410	**0.1969**	0.029	0.025
mmu-miR-665/rno-miR-665	**0.1996**	0.045	0.036
hsa-miRPlus-E1093	**0.2037**	0.031	0.027
hsa-miR-1260	**0.2093**	0.034	0.029
hsa-miR-1296	**0.2131**	0.060	0.047
mmu-miR-1900	**0.2184**	0.021	0.019
mmu-miR-743b-3p	**0.2281**	0.053	0.043
hsa-miR-494/mmu-miR-494	**0.2329**	0.011	0.011
hsa-miR-141/mmu-miR-141/rno-miR-141	**0.2373**	0.051	0.042
mmu-miR-1934	**0.2531**	0.037	0.032
hsa-miR-933	**0.2562**	0.038	0.033
ebv-miR-BHRF1-1	**0.2567**	0.039	0.034
hsa-miR-1284	**0.2647**	0.047	0.040
mmu-miR-2144	**0.2705**	0.027	0.024
hsa-miR-637	**0.2768**	0.057	0.047
hsa-miR-675*	**0.2850**	0.054	0.045

Table 2 (Continued)

mmu-miR-291b-5p	**0.2893**	0.046	0.040
hsa-miR-1275	**0.2939**	0.041	0.036
mmu-miR-300*/rno-miR-300-5p	**0.2941**	0.018	0.017
sv40-miR-S1-5p	**0.2980**	0.030	0.028
hsa-miR-422a	**0.3016**	0.048	0.041
mmu-miR-291a-5p/rno-miR-291a-5p	**0.3114**	0.044	0.038
hsa-miRPlus-E1097	**0.3115**	0.049	0.042
mmu-miR-2143	**0.3119**	0.039	0.035
hsa-miR-139-5p/mmu-miR-139-5p/rno-miR-139-5p	**0.3133**	0.042	0.037
mmu-miR-207/rno-miR-207	**0.3155**	0.021	0.019
ebv-miR-BART8*	**0.3215**	0.041	0.036
hsa-miRPlus-F1246	**0.3250**	0.019	0.018
mmu-miR-762	**0.3265**	0.092	0.072
mmu-miR-667/rno-miR-667	**0.3283**	0.050	0.044
hsa-miR-519e*	**0.3331**	0.047	0.042
hsv1-miR-H6	**0.3350**	0.064	0.054
mmu-miR-2135	**0.3384**	0.044	0.039
mmu-miR-2146	**0.3390**	0.022	0.021
hsa-miRPlus-F1240	**0.3408**	0.304	0.161
mmu-miR-1952	**0.3533**	0.044	0.039
hsa-miRPlus-E1038	**0.3546**	0.021	0.020
hsa-miRPlus-E1225	**0.3624**	0.060	0.051
hsa-miR-29c/mmu-miR-29c/rno-miR-29c	**0.3643**	0.051	0.045
mmu-miR-2141	**0.3654**	0.034	0.031
hsa-miR-1308	**0.3665**	0.041	0.037
hsa-miRPlus-F1127	**0.3670**	0.125	0.093
hsa-miR-483-3p	**0.3909**	0.039	0.035
hsa-miR-513a-5p	**0.4058**	0.038	0.035
hsa-miR-224*	**0.4072**	0.054	0.048
hsa-miR-152/mmu-miR-152/rno-miR-152	**0.4228**	0.039	0.036
hsa-miR-103-2*	**0.4295**	0.062	0.054
hsa-miRPlus-E1238	**0.4334**	0.066	0.057
hsa-miR-551b/mmu-miR-551b/rno-miR-551b	**0.4429**	0.038	0.035
hsa-miR-1280	**0.4526**	0.054	0.048
hsa-miRPlus-E1102	**0.4550**	0.067	0.058
hsa-miR-1976	**0.4551**	0.031	0.029
mghv-miR-M1-4	**0.4596**	0.032	0.030
mghv-miR-M1-3	**0.4609**	0.124	0.098
hsa-miR-1908	**0.4679**	0.065	0.057
mmu-miR-21*/rno-miR-21*	**0.4684**	0.191	0.136
mmu-miR-2140	**0.4759**	0.066	0.058

Table 2 (Continued)

hsa-miR-187*	**0.4780**	0.072	0.062
hsa-miR-490-3p/mmu-miR-490/rno-miR-490	**0.4817**	0.053	0.047
hsa-miR-617	**0.4833**	0.073	0.064
hsa-miRPlus-E1285	**0.4846**	0.062	0.055
mmu-miR-678	**0.4999**	0.090	0.076
hsa-miR-15a/mmu-miR-15a	**2.0168**	0.0718	0.0693
hsa-miR-34a/mmu-miR-34a/rno-miR-34a	**2.0396**	0.3049	0.2652
hsa-miRPlus-E1200	**2.0488**	0.1276	0.1201
hsa-miR-98/mmu-miR-98/rno-miR-98	**2.0555**	0.0888	0.0851
hsa-miR-365/mmu-miR-365/rno-miR-365	**2.0812**	0.1797	0.1654
hsa-miR-1255a	**2.0849**	0.1755	0.1619
hsa-miR-27b/mmu-miR-27b/rno-miR-27b	**2.1053**	0.0432	0.0424
hsa-miR-620	**2.1068**	0.1438	0.1346
hsa-miRPlus-F1064	**2.1144**	0.1904	0.1747
mmu-miR-466d-3p	**2.1184**	0.2845	0.2508
hsa-miR-27a/mmu-miR-27a/rno-miR-27a	**2.1217**	0.2372	0.2134
hsa-miR-181a/mmu-miR-181a/rno-miR-181a	**2.1294**	0.1448	0.1356
SNORD3@	**2.1389**	0.2015	0.1842
hsa-miR-29a/mmu-miR-29a/rno-miR-29a	**2.1643**	0.1632	0.1518
mmu-miR-466i	**2.1976**	0.1733	0.1607
mmu-miR-1897-5p	**2.2039**	0.2786	0.2473
rno-miR-352	**2.2061**	0.3208	0.2801
mmu-miR-685/rno-miR-685	**2.2232**	0.3942	0.3348
hsa-miR-659	**2.2454**	0.2094	0.1915

Table 2 (Continued)

SNORD13	2.2584	0.2523	0.2270
hsa-miR-765	2.2694	0.2028	0.1862
mmu-miR-883a-5p	2.2746	0.1534	0.1437
hsa-miR-1299	2.2988	0.1372	0.1295
mmu-miR-467e*	2.3276	0.1730	0.1610
mmu-miR-1944	2.3657	0.2552	0.2303
hsa-miRPlus-A1015	2.4493	0.4633	0.3896
hsa-miR-103/mmu-miR-103/rno-miR-103	2.4919	0.5751	0.4672
mmu-miR-467g	2.5081	0.1819	0.1696
hsa-miR-93/mmu-miR-93/rno-miR-93	2.5346	0.3935	0.3406
hsa-let-7c/mmu-let-7c/rno-let-7c	2.5500	0.2642	0.2394
hsa-miRPlus-E1232	2.5516	0.3146	0.2801
rno-miR-466c	2.5519	0.1351	0.1283
rno-miR-466b	2.5703	0.2226	0.2049
hsa-let-7d/mmu-let-7d/rno-let-7d	2.6003	0.2889	0.2601
mmu-miR-466e-5p	2.6287	0.1138	0.1091
mmu-miR-669f	2.6477	0.1976	0.1839
mmu-miR-467f	2.6522	0.7428	0.5803
hsa-let-7a/mmu-let-7a/rno-let-7a	2.6560	0.1762	0.1652
mmu-miR-466f-3p	2.6861	0.2769	0.2510
mmu-miR-1187	2.7479	0.1819	0.1706
mmu-miR-466b-5p	2.8139	0.129	0.1236

Table 2 (Continued)

hsa-let-7i/mmu-let-7i/rno-let-7i	2.8510	0.2840	0.2583
mmu-miR-805	2.8694	0.3015	0.2729
hsa-miR-92a	2.9036	0.2872	0.2614
mmu-miR-669e	2.9207	0.3617	0.3219
hsa-miRPlus-D1100/mmu-miR-674/rno-miR-674-5p	2.9445	0.4959	0.4244
mmu-miR-199b*	2.9726	0.4747	0.4094
hsa-miR-574-5p/mmu-miR-574-5p	2.9943	0.2205	0.2054
hsa-miR-214/mmu-miR-214/rno-miR-214	2.9969	0.4003	0.3532
SNORD65	3.0362	0.2388	0.2214
mmu-miR-669o	3.0455	0.3262	0.2946
mmu-miR-706	3.0467	0.1021	0.0988
mmu-miR-669l	3.0782	0.4299	0.3772
mmu-miR-466a-5p	3.0815	0.1949	0.1833
mmu-miR-690	3.0820	0.5294	0.4518
hsa-miR-106b/mmu-miR-106b/rno-miR-106b	3.0919	0.3290	0.2974
hsa-let-7b/mmu-let-7b/rno-let-7b	3.1700	0.2110	0.1979
hsa-miR-17/mmu-miR-17/rno-miR-17-5p	3.1875	0.6463	0.5374
mmu-miR-466c-5p	3.2616	0.4348	0.3837
mmu-miR-691	3.3331	0.6493	0.5434
hsa-miR-378/mmu-miR-378/rno-miR-378	3.3664	0.2925	0.2691
hsa-miR-191/mmu-miR-191/rno-miR-191	3.3957	0.3188	0.2914
hsa-miR-99b/mmu-miR-99b/rno-miR-99b	3.4281	0.346	0.3144

Table 2 (Continued)

mmu-miR-466d-5p	3.4372	0.1081	0.1048
hsa-miR-32*	3.5293	0.3086	0.2838
hsa-miR-140-3p/mmu-miR-140*/rno-miR-140*	3.5470	0.3691	0.3343
hsa-miR-199a-3p/hsa-miR-199b-3p/mmu-miR-199a-3p/mmu-miR-199b/rno-miR-199a-3p	3.5625	0.3531	0.3212
mmu-miR-669n	3.6553	0.1834	0.1746
hsa-miRPlus-E1212	3.8097	0.2111	0.2000
SNORD2	3.8944	0.3696	0.3375
hsa-miR-130a/mmu-miR-130a/rno-miR-130a	3.9705	0.2571	0.2415
SNORD38B	3.9860	0.4102	0.3719
hsa-miR-221/mmu-miR-221/rno-miR-221	4.0565	0.4706	0.4217
hsa-let-7e/mmu-let-7e/rno-let-7e	4.1168	0.3671	0.3370
RNU6-1_RNU6-2	4.1224	0.5384	0.4762
hsa-miR-210/mmu-miR-210/rno-miR-210	4.1881	0.5627	0.4960
mmu-miR-669c	4.4424	0.6467	0.5645
hsa-miR-133a/mmu-miR-133a/rno-miR-133a	4.4969	0.2633	0.2488
hsa-miR-125a-5p/mmu-miR-125a-5p/rno-miR-125a-5p	4.5242	0.4560	0.4142
hsa-miR-23a/mmu-miR-23a/rno-miR-23a	4.6073	0.6248	0.5502
hsa-miR-1/mmu-miR-1	4.8451	0.7052	0.6156
hsa-miRPlus-E1016	4.9299	1.4127	1.0980
RNU5	4.9741	1.7574	1.2986
hsa-miR-146b-5p/mmu-miR-146b/rno-miR-146b	5.0830	0.9875	0.8268
hsa-miR-22/mmu-miR-22/rno-miR-22	5.2350	0.602	0.5405

Table 2 (Continued)

hsa-miR-320d	5.2360	0.7629	0.6659
hsa-miR-24/mmu-miR-24/rno-miR-24	5.6326	0.5615	0.5106
hsa-miR-199a-5p/mmu-miR-199a-5p/rno-miR-199a-5p	5.8123	0.6513	0.5857
hsa-miR-223/mmu-miR-223/rno-miR-223	5.8920	0.6723	0.6034
hsa-miR-15b/mmu-miR-15b/rno-miR-15b	5.9905	0.4155	0.3885
hsa-miR-23b/mmu-miR-23b/rno-miR-23b	5.9965	0.4458	0.4149
hsa-miR-222/mmu-miR-222/rno-miR-222	6.3717	1.4359	1.1718
hsa-miR-142-3p/mmu-miR-142-3p/rno-miR-142-3p	7.0493	1.3006	1.0980
hsa-miR-1827	7.8660	0.6476	0.5983
mmu-miR-1949	8.0162	0.7667	0.6997
RNU1	8.2134	0.7056	0.6498
hsa-miR-16/mmu-miR-16/rno-miR-16	8.4870	0.7730	0.7084
mmu-miR-709	8.8139	1.2563	1.0995
hsa-miR-133b/mmu-miR-133b/rno-miR-133b	9.6101	0.5724	0.5402
hsa-miR-1979	9.9484	1.0422	0.9434
hsa-miR-31/mmu-miR-31/rno-miR-31	17.7694	2.8657	2.4678
hsa-miR-125b/mmu-miR-125b-5p/rno-miR-125b-5p	19.0911	1.3801	1.2871
hsa-miR-21/mmu-miR-21/rno-miR-21	26.0627	1.8453	1.7233

Table 2: miRNAs differentially expressed in a comparison between tumor and pancreas from the same control mouse that received an injection of JC101 cells. Numbers in blue represent miRNAs whose expression is lower in tumor than pancreas and orange numbers represent miRNAs whose expression is increased in the tumor compared to the pancreas.

Table 3

miRNA	Relative Quant (Tumor DER/Pancreas DER)	Pos Error	Neg Error
mmu-miR-763	**0.0498**	0.007	0.006
hsa-miR-221*	**0.0557**	0.009	0.008
kshv-miR-K12-8	**0.0935**	0.038	0.027
mmu-miR-452	**0.1067**	0.008	0.008
ebv-miR-BART2-3p	**0.1179**	0.007	0.006
hsa-miR-494/mmu-miR-494/rno-miR-494	**0.1348**	0.007	0.007
hsa-miR-30b*	**0.1600**	0.008	0.008
hsa-miR-200b/mmu-miR-200b/rno-miR-200b	**0.1721**	0.007	0.007
hsa-miR-452	**0.1725**	0.053	0.041
hsa-miR-802/mmu-miR-802/rno-miR-802	**0.1826**	0.028	0.025
hsa-miR-675*	**0.1886**	0.051	0.040
hsa-miR-200c/mmu-miR-200c/rno-miR-200c	**0.1914**	0.013	0.012
mmu-miR-675-5p/rno-miR-675	**0.2382**	0.008	0.008
hsa-miR-933	**0.2668**	0.052	0.043
hsa-miR-148a/mmu-miR-148a	**0.2925**	0.252	0.135
mmu-miR-300*/rno-miR-300-5p	**0.3029**	0.039	0.035
mmu-miR-291a-5p/rno-miR-291a-5p	**0.3095**	0.046	0.040
sv40-miR-S1-5p	**0.3313**	0.039	0.035
mmu-miR-291b-5p	**0.3377**	0.063	0.053
hsa-miR-921	**0.3414**	0.035	0.031
hsa-miR-519e*	**0.3710**	0.029	0.027
mmu-miR-667/rno-miR-667	**0.3788**	0.037	0.033
hsa-miR-520d-5p	**0.4005**	0.042	0.038
mmu-miR-325/rno-miR-325-3p	**0.4109**	0.052	0.046
hsa-miRPlus-C1115 (miRPlus_17952)	**0.4171**	0.024	0.023
hsa-miR-513a-5p	**0.4191**	0.029	0.027
hsa-miR-503	**0.4210**	0.046	0.041
mghv-miR-M1-4	**0.4307**	0.034	0.031
hsa-miR-371-5p	**0.4327**	0.031	0.029
hsa-miR-551b/mmu-miR-551b/rno-miR-551b	**0.4386**	0.042	0.038
hsa-miR-193a-5p	**0.4457**	0.028	0.026
mmu-miR-294*/rno-miR-294	**0.4513**	0.048	0.043
hsa-miR-149*	**0.4516**	0.052	0.047
hsa-miR-1908	**0.4530**	0.073	0.063
hsa-miR-617	**0.4537**	0.026	0.024
mmu-miR-351/rno-miR-351	**0.4559**	0.033	0.031
hsa-miR-518c*	**0.4608**	0.043	0.040

Table 3 (Continued)

ebv-miR-BART8*	0.4847	0.021	0.020
hsa-miR-338-5p/mmu-miR-338-5p/rno-miR-338*	0.4929	0.190	0.137
hsa-miR-665	0.4959	0.045	0.042
hsa-miR-140-3p/mmu-miR-140*/rno-miR-140*	2.0269	0.380	0.320
hsa-miR-574-5p/mmu-miR-574-5p	2.0352	0.167	0.155
mmu-miR-466d-5p	2.1196	0.033	0.032
mmu-miR-690	2.1412	0.321	0.279
hsa-miR-550	2.1695	0.072	0.070
hsa-miR-26b/mmu-miR-26b/rno-miR-26b	2.2153	0.055	0.054
hsa-miR-26a/mmu-miR-26a/rno-miR-26a	2.4059	0.247	0.224
hsa-miR-146b-5p/mmu-miR-146b/rno-miR-146b	2.4453	0.512	0.423
hsa_SNORD3@	2.4466	0.211	0.194
mmu-miR-674/rno-miR-674-5p	2.4734	0.646	0.512
hsa-miR-27a/mmu-miR-27a/rno-miR-27a	2.4786	0.687	0.538
mmu-miR-706	2.4829	0.131	0.125
mmu-let-7i/rno-let-7i	2.5771	0.492	0.413
hsa_SNORD2	2.5997	0.143	0.136
mmu-let-7g	2.6195	1.318	0.877
hsa-miR-32*	2.6377	0.119	0.114
hsa-miR-20a/mmu-miR-20a/rno-miR-20a	2.7642	0.198	0.185
hsa-miR-106b/mmu-miR-106b/rno-miR-106b	2.8863	0.549	0.461
mmu-let-7f/rno-let-7f	2.9447	2.522	1.358
hsa-let-7i/mmu-let-7i/rno-let-7i	2.9875	0.456	0.396
hsa-miR-27b/mmu-miR-27b/rno-miR-27b	3.0282	0.185	0.174
hsa-let-7a/mmu-let-7a/rno-let-7a	3.3296	0.375	0.337
hsa-miR-302d*	3.3680	0.178	0.169
mmu-miR-691	3.3778	0.796	0.644
hsa-miR-99b/mmu-miR-99b/rno-miR-99b	3.5258	0.532	0.462
hsa-miR-199a-5p/mmu-miR-199a-5p/rno-miR-199a-5p	3.7414	0.340	0.311
hsa-miR-130a/mmu-miR-130a/rno-miR-130a	3.7579	0.452	0.403
hsa-miR-191/mmu-miR-191/rno-miR-191	3.8539	0.151	0.145
mmu-let-7d/rno-let-7d	3.8730	0.324	0.299
hsa-miR-29a/mmu-miR-29a/rno-miR-29a	4.0693	0.674	0.578
hsa-miR-222/mmu-miR-222/rno-miR-222	4.1035	1.502	1.099
hsa-miR-223/mmu-miR-223/rno-miR-223	4.2059	0.688	0.591
hsa-let-7c/mmu-let-7c/rno-let-7c	4.3136	0.274	0.258

Table 3 (Continued)

hsa-miR-129*	4.6160	0.311	0.291
hsa-miRPlus-A1083 (miRPlus_42856)	4.6939	0.401	0.369
hsa-miR-133a/mmu-miR-133a/rno-miR-133a	4.7570	0.260	0.247
hsa-let-7b/mmu-let-7b/rno-let-7b	4.9793	0.474	0.433
hsa-miR-133b/mmu-miR-133b/rno-miR-133b	4.9808	0.536	0.484
hsa-miR-22/mmu-miR-22/rno-miR-22	5.1922	0.219	0.210
hsa-miR-214/mmu-miR-214/rno-miR-214	5.1967	0.486	0.444
hsa-miR-15b/mmu-miR-15b/rno-miR-15b	5.5191	0.659	0.589
hsa-miR-16/mmu-miR-16/rno-miR-16	5.5351	0.871	0.752
mmu-miR-709	5.6932	1.165	0.967
hsa-let-7e/mmu-let-7e/rno-let-7e	5.8241	0.298	0.283
hsa-miR-23a/mmu-miR-23a/rno-miR-23a	5.8662	0.479	0.443
hsa-miR-125a-5p/mmu-miR-125a-5p/rno-miR-125a-5p	6.1261	0.333	0.316
hsa-miR-23b/mmu-miR-23b/rno-miR-23b	6.1373	5.119	2.791
hsa-miR-31/mmu-miR-31/rno-miR-31	6.5310	0.282	0.271
hsa-miR-1/mmu-miR-1	6.5549	1.016	0.880
hsa-miR-129-3p/mmu-miR-129-3p/rno-miR-129*	6.7539	0.738	0.665
hsa-miR-24/mmu-miR-24/rno-miR-24	7.6734	1.152	1.001
hsa-miR-21/mmu-miR-21/rno-miR-21	15.3540	2.181	1.910
hsa-miR-125b/mmu-miR-125b-5p/rno-miR-125b-5p	25.1075	8.347	6.265

Table 3: miRNAs differentially expressed in a comparison between tumor and pancreas from the same DER mouse that received an injection of JC101 cells. Numbers in blue represent miRNAs whose expression is lower in tumor than pancreas and orange numbers represent miRNAs whose expression is increased in the tumor compared to the pancreas.

Altered miRNA expression found in a comparison of DER pancreas and control pancreas yielded fewer miRNAs with altered expression (Table 4) than were seen in the cancer versus normal tissue described above. However, among the altered miRNAs were mir-155, 216, and 217 all of which have previously been identified in miRNA profiles of pancreatic cancer derived from paraffin-embedded human tissues. Of particular interest is mir-155, whose overexpression is associated with the early stages of pancreatic carcinogenesis [15]. Increased expression of mir-216 and -217 have been associated with increased survivability in human pancreatic cancer

cases when found with a lower expression of mir-196 [16]. Though mir-196 was not seen to be altered in our pilot study, a follow up on the importance of this expression profile is warranted. Surprisingly, the comparison of DER tumor and control tumor in our follow-up study (n=3/diet) yielded the fewest differentially expressed miRNAs (Table 5). However, it is important to note that all three miRNA identified in the follow-up study also appeared in the pilot study.

miRNA	Relative Quant (Pancreas DER / Pancreas Control)	Pos Error	Neg Error
hsa-miR-422a	0.420105971	0.038	0.035
hsa-miR-155	0.420193555	0.070	0.060
hsa-miR-1308	0.425156062	0.016	0.016
hsa-miRPlus-E1038	0.436275487	0.047	0.043
ebv-miR-BART6-3p	0.438015899	0.039	0.035
mmu-miR-2146	0.46530473	0.052	0.047
hsa-miR-217/mmu-miR-217/rno-miR-217	2.013822449	0.244	0.217
hsa-miRPlus-F1246	2.380355076	0.281	0.251
hsa-miR-216b/mmu-miR-216b	2.568190459	0.650	0.519

Table 4: miRNAs differentially expressed in a comparison between DER and control pancreas from mice that received an injection of JC101 cells. Numbers in blue represent miRNAs whose expression is lower in DER pancreas when compared to control pancreas and orange numbers represent miRNAs whose expression is increased in DER pancreas compared to control pancreas.

miRNA	Relative Quant (Tumor DER / Tumor Control)	Pos Error	Neg Error
mmu-miR-2135	0.40967635	0.033	0.031
mmu-miR-2146	0.433223198	0.031	0.029
mmu-miR-669c	0.491028809	0.108	0.089

Table 5: miRNAs differentially expressed in a comparison between DER and control tumor from mice that received an injection of JC101 cells. Numbers in blue represent miRNAs whose expression is lower in DER tumor when compared to control tumor.

In light of the ability of the Exiqon array system to successfully detect altered miRNA expression, JC101 tumors that from DER (n=3) and control (n=3) mice were paired and had their total RNA extracted and miRNA expression analyzed as described above. Though a variable number of miRNA were expressed in each sample (Appendix), three miRNA had their expression consistently decreased in the DER tumors when compared to control tumors, though only mir-669c has a known function (Fig.5). Interestingly, mir-669c has been shown in a number of studies to increase as a mouse ages and targets several classes of *glutathione S*-transferases, including Mgst1. Given the relationship between DER and an increased life span seen in studies, the role that mir-669c is playing in the tumor system warrants further investigation[17].

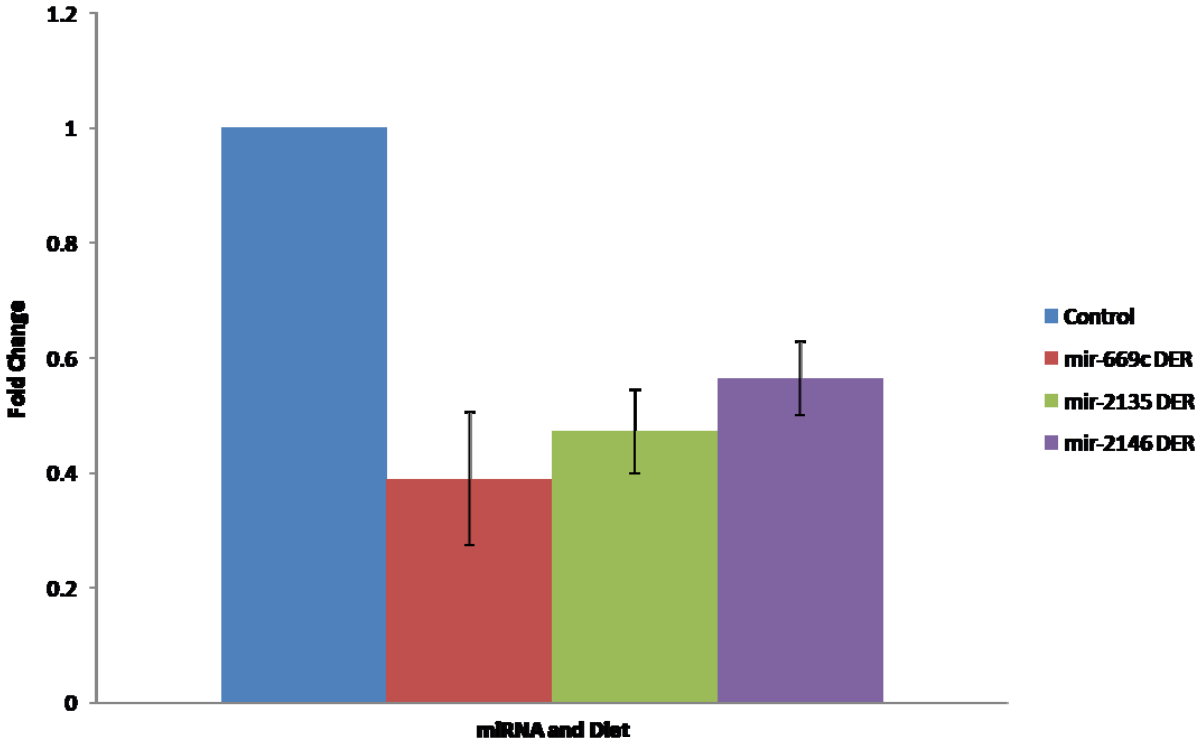

Figure 5: Effects of DER on miRNA expression in JC101 Tumors. Exiqon miRNA arrays were performed on three sets of matched DER and control tumors. Analysis of the data showed that 3 miRNA were consistently down regulated compared to control. Expression of miRNA-669c was reduce by an average of 61% compared to control (p=0.031). Expression of mir-2135 was reduced by an average of 53% of compared to control (p=0.039). Expression of mir-2146 was reduced by an average of 44% when compared to control (p=0.014)

Further investigation of miRNA will utilize TaqMan MicroRNA Reverse Transcription Kit and Taqman miRNA Probes (Applied Biosystems). However, before proceeding with RT-PCR for miRNA one must determine the appropriate control to use. Based on literature searches mir-16 and snU6 were selected for evaluation in a series of serum starvation and IGF-1 treatment experiments with Panc02 cells. Upon analysis of the data mir-16 appears to be more stably expressed than snU6 (Table 6) and thus will be selected for use as a control in future qPCR experiments.

snU6	1 hr	2 hr	4 hr	8 hr	Complete	Serum Free
Average	25.22	25.18	25.85	23.72	24.97	24.06
St Dev	0.7339	1.446	1.349	0.3355	2.471	1.497
SEM	0.2996	0.5904	0.5507	0.1370	1.009	0.6112

mir-16	1 hr	2 hr	4 hr	8 hr	Complete	Serum Free
Average	22.52	23.66	22.45	23.03	22.82	23.12
St Dev	0.3170	0.9423	0.7830	0.3535	0.4066	0.4061
SEM	0.1294	0.3847	0.3197	0.1443	0.1660	0.16579

Table 6: Determination of control for RT-PCR of miRNA. RT-PCR was performed to screen for a control for future work with miRNA. Mir-16 was determined to be a more suitable control for future experiments due to its less varied expression over time and in different condition.

Chapter 4: Discussion and Future Directions

Expanding our understanding of the mechanisms by which DER hinders pancreatic cancer growth and progression has the potential to provide insights into combating the disease. Here we show the feasibility of a subcutaneous syngeneic transplant of JC101 cells in FVB mice. Consistent with previous findings from our lab and others, DER suppressed JC101 pancreatic tumor growth, decreased serum levels of several hormones and growth factors linking metabolism and cell growth, and decreased cell proliferation, fibrosis and vascularization of the tumors[8, 10, 18, 19]. These findings suggest that this is a valid model for further exploring the mechanisms underlying the effects of DER on pancreatic tumor growth, including miRNA analyses.

In contrast, we found no effect of DER on NB508 tumor growth. Surprisingly, subcutaneous tumor growth following transplantation of these cells, which are driven by overexpression K-ras in combination with INK-4A deficiency, was much less than that observed with JC101 cells. It is possible that more robust tumor growth with these cells requires a higher cell concentration, longer follow-up, or the presence of support materials, such as the use of matrigel. Given the importance of K-ras mutations in human pancreatic cancer, additional experiments are warranted with these NB508 cells to determine what conditions, if any, are required to optimize tumor growth following subcutaneous transplantation. However, such studies are beyond the scope of this thesis, and all subsequent analyses will focus on the JC101 cells, which display a robust tumor response that is suppressed by DER.

To explore the potential role of miRNA in the effects of DER on JC101 tumor growth, array data were obtained from matched tumor tissue using the Exiqon array platform. This analysis revealed that three miRNAs were consistently down regulated by DER; mir-669c, mir-

2135, and mir-2146. Only mir-669c has been previously identified, with mir-2135 and 2146 being computer predicted miRNAs, with no known function at present. The down regulation of mir-669c by DER is of great interest in light of its known role in regulating translation of glutathione-s transferase (GST) [20]. GSTs are a family of enzymes composed of many cytosolic, mitochondrial, and microsomal proteins that act as catalysts for many important cellular reactions linked to aging and cancer. They as also impact the metabolism of many endogenous and xenobiotic substrates[21]. Given the wide range or roles that GSTs play in the body, including detoxification, oxidative stress, protein transport, it is not surprising that GSTs have been shown to play a role in carcinogenesis[20]. With respect to pancreatic cancer, a recent epidemiological study found that mutations in GST increased the odds ratio of pancreatic cancer occurring in a patient to 1.38-2.50 depending on the mutation[22]. The known functionality of mir-669c as a regulator of GST's, combined with the observation that mir-669c expression increases with age (a key risk factor for pancreatic cancer) suggests that this miRNA may play an important role in carcinogenesis [5, 17]. Though substantial work has been reported concerning GST's and related pathways in cancer, no prior studies have shown connections between energy balance, microRNAs,(including mr669c), and pancreatic cancer.

Despite the obvious limitations inherent in the small sample size, the data obtained from my initial pilot to assess the usefulness of the Exiqon array platform also warrants further analyses. Comparisons between control tumor and pancreas, as well DER tumor and pancreas, yielded a large number of differentially expressed miRNA that need extensive follow up work in order to identify possible avenues for future research that may have relevance to diet and pancreatic cancer prevention. The analysis of differential miRNA expression between DER and control pancreas yielded a small profile with three interesting results. Mir-155 overexpression is

thought to be an important early step in pancreatic carcinogenesis, with upwards of 80% of patients displaying overexpression in this miRNA[15]. Giving the role, that upregulation of mir-155 plays in early carcinogenesis it is of note that the pancreas from the DER-treated mouse had a decreased expression of mir-155 compared to control. If confirmed in larger studies, regulation of mir-155 in normal pancreas may be a means by which energy balance modifies risk for pancreatic cancer in patients. Also of note is the upregulation of mir- 216 and 217 by DER in pancreas when compared to control. Mir-216 and 217 are often used as an indicator of prognosis in combination with mir-196a. In general an increase in expression of mir-196a and a decrease in the expression of mir-216 and 217 is associated with a poor prognosis[16]. However, mir-196a did not appear to be differentially regulated, and the increase in mir-216 and 217 expression may be indicative of calorie restriction lending itself to a better prognosis. It is important to note however, that findings involving mir-155, -216, and -217 are at best preliminary at this time given the sample size of one. Further evaluation of the state of the miRNAs in normal and DER pancreas is necessary to determine if these results occur consistently, and thus warrant further research.

Given the global effects of DER we were surprised by the small number of miRNA that were differentially regulated in matched tumor tissue. The most likely explanation for the phenomena is that the JC101 cell transplant model is not ideal for determining the relationship between DER, cancer, and miRNA. Many studies have shown that miRNA alteration occurs early in the tumorigenesis process rather than later[23]. Therefore, the use of transformed cells with a large number of pre-existing mutations may have hindered DER's ability to alter miRNA expression. The best way to assess this hypothesis is to use a transgenic model with tissue collection at multiple timepoints, allowing a comparison of miRNA expression over time. A

better understanding of the timeline of differential miRNA expression in pancreatic cancer has the potential to elucidate new targets for diagnostic tests as well lead to the development of more effective treatment and/or prevention strategies.

Appendix

Description	D10001	D09071402 Caloric Restriction
Ingredient (gm)		
Casein, 80 Mesh	200	200
DL-Methionine	3	3
Fruit and Veggie Blend, FutureCeuticals	0	0
Sucrose	500	275
Corn Starch	150	82.3
Cellulose	50	50
Corn Oil	50	50
Olive Oil	0	0
Menhaden Oil (with 200 ppm tBHQ)	0	0
tBHQ	0	0
Mineral Mix S10001	35	35
Vitamin Mix V10001	10	10
Choline Bitartrate	2	2
Celebrex (75% celecoxib)	0	0
FD&C Yellow Dye #5	0	0.04
FD&C Red Dye #40	0	0.01
FD&C Blue Dye #1	0	0
Total	1000	707.35
Diet #		
gm		
Protein	203.0	203.0
Carbohydrate	660.0	367.3
Fat	50.0	50.0
Fiber	50.0	50.0
gm%		
Protein	20.3	28.7
Carbohydrate	66.0	51.9
Fat	5.0	7.1
Fiber	5.0	7.1
kcal		
Protein	812	812
Carbohydrate	2640	1469
Fat	450	450
Total	3902	2731
kcal%		
Protein	21	30
Carbohydrate	68	54
Fat	12	16
Total	100	100
kcal/gm	3.9020	3.86
To feed a 30% caloric restriction, feed this many grams of caloric restriction diet per 1 gram of each of the other diets	0.71	
gm		
Calcium	5.180	5.180
Copper	0.006	0.006
Iron	0.045	0.045
Magnesium	0.501	0.501
Manganese	0.059	0.059
Phosphorus	3.990	3.990
Potassium	3.605	3.605
Selenium	0.000	0.000
Sodium	1.000	1.000
Zinc	0.029	0.029

AIN-76A Rodent Diet and Modification For 30 % Caloric Restriction

Name	Relative Quant (Control/DER)	Pos. Error	Neg. Error
mmu-miR-106a	0.416	0.086	0.072
mmu-miR-101a	0.422	0.085	0.071
mmu-miR-30d	0.436	0.077	0.065
mmu-miR-301a	0.438	0.071	0.061
mmu-miR-140*	0.461	0.205	0.142
mmu-miR-191	0.486	0.041	0.038
mmu-miR-195	0.487	0.038	0.035
mmu-miR-24	0.489	0.020	0.020
mmu-miR-210	0.498	0.043	0.039
hsa-miRPlus-E1151	2.030	0.254	0.226
mmu-miR-691	2.032	0.258	0.229
mmu-miR-709	2.060	0.086	0.083
hsa-miR-32*	2.076	0.382	0.323
hsa-miR-765	2.102	0.314	0.273
hsa-miR-149*	2.140	0.309	0.270
hsa-miR-617	2.149	0.089	0.085
mmu-miR-669n	2.207	0.235	0.212
mmu-miR-466d-5p	2.232	0.125	0.119
hsa-miRPlus-F1225	2.245	0.230	0.208
hsa-miRPlus-E1212	2.289	0.275	0.246
mmu-miR-1196	2.384	0.075	0.073
mmu-miR-1897-5p	2.410	0.279	0.250
mmu-miR-669c	2.505	0.293	0.262
mmu-miR-300*	2.604	0.255	0.232
hsa-miR-422a	2.909	0.404	0.355
mmu-miR-2135	3.008	0.322	0.291
hsa-miRPlus-F1193	3.282	0.336	0.305

miRNA analysis of first matched DER and Control Tumor

Name	Relative Quant (Control/DER)	Pos. Error	Neg. Error
mmu-miR-21	0.346	0.029	0.027
mmu-miR-19b	0.362	0.052	0.045
mmu-miR-222	0.376	0.030	0.028
mmu-miR-130a	0.385	0.042	0.038
mmu-miR-31*	0.390	0.024	0.023
mmu-miR-29b	0.397	0.040	0.037
mmu-miR-193	0.414	0.062	0.054
mmu-miR-155	0.426	0.068	0.059
mmu-miR-106a	0.449	0.037	0.034
mmu-miR-31	0.452	0.061	0.054
mmu-miR-210	0.454	0.071	0.061
hsa-miR-1979	0.474	0.032	0.030
mmu-miR-301a	0.480	0.039	0.036
mmu-miR-221	0.481	0.031	0.029
mmu-miR-20a	0.491	0.032	0.030
mmu-miR-23a	0.498	0.026	0.025
hsa-miR-1299	2.051	0.211	0.191
mmu-miR-468	2.101	0.159	0.148
hsa-miRPlus-F1225	2.115	0.068	0.065
mmu-miR-378	2.128	0.160	0.149
mmu-miR-2146	2.170	0.284	0.251
hsa-miRPlus-E1151	2.174	0.165	0.153
hsa-miR-422a	2.215	0.344	0.298
hsa-miRPlus-F1193	2.233	0.301	0.266
mmu-miR-467h	2.238	0.192	0.177
mmu-miR-883a-5p	2.276	0.269	0.240
mmu-miR-300*	2.304	0.256	0.231
mmu-miR-1897-5p	2.319	0.244	0.221
hsa-miRPlus-E1200	2.391	0.073	0.070
mmu-miR-466f-5p	2.393	0.314	0.278
mmu-miR-466e-5p	2.454	0.297	0.265
mmu-miR-1187	2.482	0.122	0.116
rno-miR-466c	2.532	0.498	0.416
mmu-miR-2135	2.619	0.135	0.128
mmu-miR-669l	2.627	0.236	0.216
mmu-miR-466b-5p	2.670	0.158	0.149
mmu-miR-466a-5p	2.763	0.163	0.154
mmu-miR-669e	2.778	0.119	0.114
mmu-miR-669n	2.803	0.151	0.143
hsa-miR-32*	2.808	0.191	0.179
mmu-miR-669o	2.876	0.187	0.176
mmu-miR-574-5p	2.878	0.315	0.284
rno-miR-466b	2.987	0.319	0.288
mmu-miR-466c-5p	3.073	0.387	0.343
mmu-miR-466d-5p	3.246	0.590	0.499

hsa-miRPlus-E1212	**3.346**	0.599	0.508
mmu-miR-669c	**3.669**	0.290	0.269
mmu-miR-133a	**3.706**	0.306	0.283
mmu-miR-1	**4.962**	0.740	0.644
mmu-miR-133b	**6.894**	0.448	0.421

miRNA analysis of second matched DER and Control Tumor

Name	Relative Quant (Control/DER)	Pos. Error	Neg. Error
hsa-miR-491-3p	0.480	0.085	0.072
hsa-miRPlus-F1193	2.003	0.259	0.230
hsa-miR-422a	2.013	0.223	0.201
mmu-miR-669c	2.016	0.203	0.184
mmu-miR-466d-5p	2.016	0.707	0.523
mmu-miR-720	2.031	0.102	0.098
mmu-miR-2132	2.232	0.152	0.143
mmu-miR-2138	3.203	0.182	0.172

miRNA analysis of third matched DER and Control Tumor

References

1. Ahmedin Jemal, R.S., Elizabeth Ward, Yongping Hao, Jiaquan Xu and Michael J. Thun, *Cancer Statistics, 2009.* CA: A Cancer Journal for Clinicians 2009. **59**(4): p. 225-229.
2. Bardeesy, N. and R.A. DePinho, *Pancreatic cancer biology and genetics.* Nat Rev Cancer, 2002. **2**(12): p. 897-909.
3. Hezel, A.F., et al., *Genetics and biology of pancreatic ductal adenocarcinoma.* Genes Dev, 2006. **20**(10): p. 1218-49.
4. Schlosser, W., et al., *Cyclooxygenase-2 is overexpressed in chronic pancreatitis.* Pancreas, 2002. **25**(1): p. 26-30.
5. Staff, M.C. *Pancreatic Cancer: Risk Factors*. 2010 April 2010 [cited 2010 November]; Available from: http://www.mayoclinic.com/health/pancreatic-cancer/DS00357/DSECTION=risk-factors.
6. Calle, E.E., et al., *Overweight, obesity, and mortality from cancer in a prospectively studied cohort of U.S. adults.* N Engl J Med, 2003. **348**(17): p. 1625-38.
7. Hedley, A.A., et al., *Prevalence of overweight and obesity among US children, adolescents, and adults, 1999-2002.* Jama, 2004. **291**(23): p. 2847-50.
8. Hursting, S.D., et al., *Energy balance and carcinogenesis: underlying pathways and targets for intervention.* Curr Cancer Drug Targets, 2007. **7**(5): p. 484-91.
9. Hursting SD, S.S., Lashinger LM, Harvey AE, Perkins SN., *Calories and carcinogenesis: lessons learned from 30 years of calorie restriction research.* Carcinogenesis, 2010. **31**(1): p. 83-9.
10. Roebuck, B.D., K.J. Baumgartner, and D.L. MacMillan, *Caloric restriction and intervention in pancreatic carcinogenesis in the rat.* Cancer Res, 1993. **53**(1): p. 46-52.
11. DP., B., *MicroRNAs: target recognition and regulatory functions.* Cell, 2009. **136**(2): p. 215-33.
12. Koturbash I, Z.F., Pogribny I, Kovalchuk O., *Small molecules with big effects: The role of the microRNAome in cancer and carcinogenesis.* Mutation Research/Genetic Toxicology and Environmental Mutagenesis, 2010.
13. Heneghan HM, M.N., Kerin MJ., *Role of microRNAs in obesity and the metabolic syndrome.* Obesity Reviews. **11**(5): p. 354-361.
14. Mark Bloomston, W.L.F., Fabio Petrocca,Stefano Volinia, Hansjuerg Alder,John P. Hagan,Chang-Gong Liu,Darshna Bhatt, Cristian Taccioli, Carlo M. Croce, *Pancreatic Adenocarcinoma From Normal Pancreas and MicroRNA Expression Patterns to Differentiate Chronic Pancreatitis.* JAMA, 2007. **297**(17): p. 1901-1908.
15. Ryu JK, H.S., Karikari CA, Hruban RH, Goggins MG, Maitra A., *Aberrant MicroRNA-155 expression is an early event in the multistep progression of pancreatic adenocarcinoma.* Pancreatology. **10**(1): p. 66-73.
16. Szafranska AE, D.T., John J, Cannon T, Sipos B, Maghnouj A, Labourier E, Hahn SA., *MicroRNA expression alterations are linked to tumorigenesis and non-neoplastic processes in pancreatic ductal adenocarcinoma.* Oncogene, 2007. **26**(30): p. 4442-52.
17. Maes OC, A.J., Sarojini H, Wang E., *Murine microRNAs implicated in liver functions and aging process.* Mech Ageing Dev., 2008. **129**(9): p. 534-41.

18. Craven-Giles, T., et al., *Dietary modulation of pancreatic carcinogenesis: calories and energy expenditure.* Cancer Res, 1994. **54**(7 Suppl): p. 1964s-1968s.
19. Tsugane S, I.M., *Insulin resistance and cancer: epidemiological evidence.* Cancer Science, 2010. **101**(5): p. 1073-9.
20. Ruzza P, R.A., Rossi CR, Floreani M, Quintieri L., *Glutathione transferases as targets for cancer therapy.* Anticancer Agents Med Chem, 2009. **9**(7): p. 763-77.
21. D Sheehan, G.M., V M Foley, and C A Dowd, *Structure, function and evolution of glutathione transferases: implications for classification of non-mammalian members of an ancient enzyme superfamily.* Journal of Biochemistry, 2001. **360**(Part 1): p. 1-16.
22. Jiao L, B.M., Hassan MM, Chang DZ, Abbruzzese JL, Evans DB, Smolensky MH, Li D., *Glutathione S-transferase gene polymorphisms and risk and survival of pancreatic cancer.* Cancer, 2007. **109**(5): p. 840-8.
23. TD., S., *Regulation of microRNA processing in development, differentiation and cancer.* J Cell Mol Med., 2008. **12**(5B): p. 1811-9.